RAPGEF2 mediates oligomeric Aβ-induced synaptic loss and cognitive dysfunction in Alzheimer's disease

You-Na Jang
Korea Brain Research Institute
HoChung Jang
Korea Brain Research Institute
Gyu Hyun Kim
Korea Brain Research Institute
Jeong-Eun Noh
Korea Brain Research Institute
Keun-A Chang
Gachon University
KEA JOO LEE (relaylee@kbri.re.kr)
Korea Brain Research Institute https://orcid.org/0000-0002-1366-4709

Research

Keywords: Alzheimer's disease, amyloid-beta, synapse, memory, GTPase, Rap

Posted Date: January 2nd, 2020

DOI: https://doi.org/10.21203/rs.2.19961/v1

Abstract

Background: Excessive neuronal activity promotes amyloid-β (Aβ) production in the brain. The Aβ oligomer triggers synaptic degeneration that precedes plaque and tangle pathology. However, the signaling molecules that link Aβ oligomers to synaptic pathology remain unclear. RAPGEF2, a guanine-nucleotide exchange factor for the small GTPase Rap, plays a role in activity-dependent synapse remodeling and is involved in the pathogenesis of epilepsy commonly observed in Alzheimer's disease (AD) patients and mouse models. Thus, we postulated that the perturbation of the RAPGEF2 signal may contribute to Aβ oligomer-induced synaptopathy in AD.

Methods: To investigate the potential role of RAPGEF2 in Aβ oligomer-induced synaptic and cognitive impairments in AD, we utilized a combination of approaches including biochemistry, molecular cell biology, light and electron microscopy, behavioral tests with primary neuron cultures, multiple AD mouse models and postmortem human AD brain tissue.

Results: We observed significantly elevated RAPGEF2 levels in the postmortem human AD hippocampus. RAPGEF2 levels also increased in the transgenic AD mouse models, generating high levels of Aβ oligomers before exhibiting synaptic and cognitive impairment. RAPGEF2 upregulation activated its downstream effectors Rap2 and JNK. In cultured hippocampal neurons, oligomeric Aβ treatment increased the fluorescence intensity of RAPGEF2 and reduced the number of dendritic spines, while silencing RAPGEF2 expression blocked Aβ oligomer-induced spine loss. Additionally, the in vivo knockdown of RAPGEF2 expression in the AD hippocampus prevented cognitive deficits and the loss of excitatory synapses.

Conclusions: These findings demonstrate that the upregulation of RAPGEF2 levels mediates Aβ oligomer-induced synaptic and cognitive disturbances in the AD hippocampus. We propose that early intervention regarding RAPGEF2 expression may have beneficial effects on early synaptic pathology and memory loss in AD.

Background

Alzheimer's disease (AD) is the most common and devastating type of dementia, with no treatment currently available to halt its progression. A number of studies support the assumption that AD is the result of synaptic failure [1, 2] and that soluble amyloid-β (Aβ) oligomers cause AD synaptic and behavioral pathogenesis [3, 4]. Indeed, synaptic dysfunction precedes Aβ plaque and neurofibrillary tangle pathology, as well as cognitive impairments in AD [5, 6]. While synapse dysfunction and memory impairments correlate poorly with plaque burden, soluble Aβ oligomer levels and synaptic aberrations are thought to be the best correlates of the early stage of memory loss in AD [7, 8]. Several lines of evidence indicate that Aβ oligomer levels are markedly elevated in the brains of AD patients and in AD mouse models expressing human-mutant amyloid precursor protein (APP) [9, 10] and that these elevated levels trigger synaptic degeneration at the level of dendritic spines [11, 12], which are tiny membrane

protrusions that receive most of the excitatory inputs in the brain [13]. It has also been suggested that excessive neuronal activity related to stress or seizures promotes Aβ production in the brain [14–16]. Together, these studies highlight the crucial role of Aβ oligomers in initiating synaptopathy and early memory loss in AD [17]. However, the signaling molecules that link Aβ oligomers to synaptic pathology are not well understood.

Rap proteins, one of the Ras families of small GTPases, play pivotal roles in neural development and synaptic plasticity in the brain [18–21]. RAPGEF2 (also named CNrasGEF, nRapGEP, PDZ-GEF1 and RA-GEF-1) is a neural-specific activator of Rap1 and Rap2 [22, 23] and associates with the synaptic scaffolding protein S-SCAM [24]. Early studies have shown that RAPGEF2-Rap signaling is involved in the activity-dependent remodeling of dendritic spines, AMPA receptor trafficking, and synaptic plasticity [21, 25–28]. Notably, a recent genetic study identified that RAPGEF2 is involved in the pathogenesis of epilepsy [29]. Because a high incidence of seizure is commonly observed in AD patients and AD mouse models [30–32], and neuronal hyperactivity increases Aβ production in vitro and in vivo [14–16], we postulated that the dysregulation of RAPGEF2 may contribute to the process of synaptic degeneration observed in AD.

Here, we report that RAPGEF2 acts as a molecular link between Aβ oligomers and synaptic aberrations. We observed that RAPGEF2 levels were highly upregulated in the postmortem human AD hippocampus and in multiple AD mouse models generating high levels of Aβ oligomers. This Aβ oligomer-mediated stimulation of RAPGEF2 activated its downstream targets Rap2 and JNK (c-Jun N-terminal kinases) in vivo. In cultured hippocampal neurons, the treatment of Aβ oligomers increased the fluorescence intensity of RAPGEF2, with a concomitant reduction in spine numbers and disruption in synaptic morphology compared to those of controls. Importantly, silencing RAPGEF2 expression prevented Aβ oligomer-induced synaptic and cognitive impairments. Taken together, our data suggest that early intervention regarding RAPGEF2 expression may provide a potential option to help mitigate synaptic and cognitive dysfunctions in AD.

Methods

Antibodies and reagents

The following antibodies were used in this study: rabbit polyclonal RAPGEF2 (#A301-966A, Bethyl Laboratories), mouse polyclonal RAPGEF2 (#H00009693-A01, Abnova), mouse monoclonal RAPGEF2 (#H00009693-M01, Abnova), mouse monoclonal Rap2 (#610216, BD Biosciences), and mouse monoclonal GFP (#ab1218, Abcam). Antibodies against phospho-p38 (#4511), p38 (#9212), phospho-JNK (#9255), JNK (#9252), Rap1 (#2399), and β-tubulin (#2146) were purchased from Cell Signaling Technology. The rabbit polyclonal GFP antibody (#A11122) and Alexa 488, 594, and 555 conjugated goat/donkey anti-mouse/rabbit secondary antibodies were obtained from Invitrogen.

Oligomeric Aβ preparation

To prepare Aβ oligomers, lyophilized β-amyloid (1–42) peptide powder was purchased from AnaSpec. According to the manufacturer's protocol, β-amyloid peptide was dissolved in 20 mM HEPES/150 mM NaCl (pH 7.2) at a concentration of 50 μM and sonicated until completely solubilized. Oligomers were acquired by diluting the Aβ peptide solution to 25 μM with phenol red-free DMEM-F12 (Caisson Labs) and incubating the diluted Aβ solution at 4 °C for 24 hrs.

Primary hippocampal neuron culture and transfection

Primary rat hippocampal cultures were prepared from embryonic day (E) 18–19 Sprague-Dawley fetal rats as previously described [25]. Briefly, after dissecting out hippocampal tissue, trypsinized cells were dissociated by triturating gently with flame-polished Pasteur pipettes. Cells were seeded on a precoated plate with poly-D-lysine (100 μg/mL, Sigma-Aldrich) and laminin (2 μg/mL, Roche) at a density of 4–5 × 10^4 cells/well. The neurons were grown in Neurobasal medium (Gibco) supplemented with SM1 (Stem Cell Technologies), 0.5 mM glutamine and 25 μM glutamate for 18–21 days in vitro (DIV). For transfections, DNA constructs were transfected into hippocampal neurons (18–21 DIV) using Lipofectamine 2000 reagent (Thermo Fisher Scientific) for 2–3 days.

Human brain tissue preparation

The human hippocampal tissue samples used in this study were obtained from the Netherlands Brain Bank (Project #1009, Amsterdam, Netherland). Experiments using human tissue were approved by the Institutional Review Board at the Korea Brain Research Institute (201610-BR-004-01). The hippocampal samples were stored at − 80 °C until use. Information about the human tissue used in this study is provided in Table 1.

Table 1

Postmortem human hippocampal samples

Group	No.	Clinical Diagnosis	Gender	Age
Controls	1	Nondemented control	M	89
	2	Nondemented control	F	92
	3	Nondemented control	F	78
	4	Nondemented control	F	60
	5	Nondemented control	F	93
	6	Nondemented control	F	82
	7	Nondemented control	M	73
	8	Nondemented control	F	72
AD patients	1	Alzheimer's disease	F	85
	2	Alzheimer's disease	M	60
	3	Alzheimer's disease	M	84
	4	Alzheimer's disease	M	74
	5	Alzheimer's disease	F	61
	6	Alzheimer's disease	F	71
	7	Alzheimer's disease	F	91
	8	Alzheimer's disease	M	81
	9	Alzheimer's disease	F	88
	10	Alzheimer's disease	F	78
	11	Alzheimer's disease	F	90
	12	Alzheimer's disease	M	78

The table shows the characteristics of the human (control and AD) individuals whose brain tissue was analyzed in the present study.

Western blot analysis

Cultured hippocampal neurons and brain tissue from mice and humans were lysed in ice-cold RIPA buffer (150 mm NaCl, 10 mm Na_2HPO_4, pH 7.2, 0.5% sodium deoxycholate, and 1% Nonidet P-40) containing a protease inhibitor cocktail (GenDepot) and a phosphatase inhibitor cocktail (Sigma-Aldrich). The lysates were centrifuged at 15,000 × g at 4 °C for 20 min. Protein concentrations of supernatants were determined

using a BCA reagent (Thermo Fisher Scientific). The samples were separated on 8–12% polyacrylamide gels, transferred to a nitrocellulose membrane (GE Healthcare Life Sciences), and blocked with 5% nonfat dry milk or 3% bovine serum albumin (Sigma-Aldrich) in 1XTBS buffer solution containing 0.1% Tween-20. Blots were incubated with primary antibodies at 4 °C overnight, followed by horseradish peroxidase-conjugated secondary antibodies (Cell Signaling Technology) or infrared dye-conjugated secondary antibodies (Li-Cor Bioscience) at room temperature for 1 hr. Blots were visualized by a Fusion Fx7 ECL system (Vilber) or an Odyssey CLx Infrared Imaging System (Li-Cor Bioscience). Protein band intensities in the western blot were quantitatively measured using ImageJ software (National Institutes of Health).

Active Rap pull-down assay

Mouse cortical tissue was homogenized in ice-cold RIPA buffer containing a protease inhibitor cocktail (GenDepot) and a phosphatase inhibitor cocktail (Sigma-Aldrich). After collecting supernatants from brain homogenates by centrifugation, lysates (1.5 mg) were incubated with 40 µl RalGDS RBD agarose beads (Abcam) at 4ºC for 3 hrs. Pellets were washed three times and resuspended in 40 µl 2X reducing SDS sample buffer (62.5 mM Tris-HCl, pH 6.8, 2% SDS, 10% glycerol, 0.1% bromophenol blue, 0.5% β-mercaptoethanol). GTP-bound active Rap1 and Rap2 levels were detected by western blotting.

Immunocytochemistry

Primary hippocampal neurons were fixed with 4% paraformaldehyde and 4% sucrose for 15 min. For the immunofluorescence labeling of RAPGEF2, neurons were fixed with 1% paraformaldehyde, followed by methanol (-20 °C). Neurons were incubated with primary antibodies in a GDB solution (30 mM phosphate buffer, pH 7.4, containing 0.1% gelatin, 0.3% Triton X-100, 450 mM NaCl) at 4 °C overnight and, then, with Alexa 488- and Alexa 594-conjugated secondary antibodies (Thermo Fisher Scientific) at room temperature for 1 hr; neurons were then mounted on a glass slide with VECTASHIELD mounting solution (Vector Labs). For the analysis of dendritic spine structures and immunofluorescence intensity, we focused on linear secondary dendritic segments of pyramidal neurons (at least 30 µm in length). The images were acquired with a TI-RCP confocal microscope (Nikon). The immunofluorescence intensity was quantified using MetaMorph Software (Molecular Devices).

Animals

All mutants and their corresponding control mice were purchased from Jackson Laboratory. The 3xTg-AD transgenic mice (MMRRC Stock No: 34830-JAX) were maintained as homozygotes. The 5xFAD mice (MMRRC Stock No: 34840-JAX) were maintained as hemizygotes by crossing with WT mice on a C57BL/6J X SJL background strain. To generate rTg (TauP301L) 4510 mice, tetO-MAPT*P301L mice (FVB-Fgf14Tg(tetO-MAPT*P301L)4510Kha/JlwsJ, Stock No. 015815) were crossed with mice from the CaMKII-tTA mouse line (B6.Cg-Tg(Camk2a-tTA)1Mmay/DboJ, Stock No. 007004). All mice were housed 4 to 5 per cage in a room maintained at 21 ± 1 °C, with an alternating 12 hrs light-dark cycle and free access to food and water.

shRNA constructs and virus production

The following oligonucleotides (5’-3’) were inserted into the pLL 3.7 vector, which simultaneously expresses RNAi-inducing shRNAs and GFP under the U6 and CMV promoters, respectively (Rubinson et al., 2003): scrambled shRNA, GCAAACGCT CGACATTAA; rat RAPGEF2-shRNA, GGACCCAACATTCATAGA (NM_001107684.1; 709–726 bp); and mouse RAPGEF2-shRNA, GCTGGAACCATTGTGTTA (NM_001099624.3; 520–537 bp). Lentiviral particles were produced according to the manufacturer’s directions (ViraPower Lentiviral Expression System, Thermo Fisher Scientific). Briefly, a mixture of plasmids was transfected into HEK293FT packaging cells. The virus-containing medium was harvested 48 or 72 hrs after transfection and subsequently precleaned with 3,000 × g centrifugation and 0.45 μm filtration (Merck Millipore). The virus-containing medium was overlaid on a sucrose-containing buffer and centrifuged at 120,000 × g at 4 °C for 2 hrs. After ultracentrifugation, supernatants were carefully removed and resuspended in phosphate buffered saline.

Stereotaxic virus injection

Two-month-old nontransgenic B6129SF2/J control and 3xTg-AD transgenic mice were anaesthetized with isoflurane, and 1 μL of the viral solution was injected bilaterally into the hippocampal CA1 region with a glass pipette at a flow rate of 0.2 μL/min according to stereotaxic coordinates (Bregma: antero-posterior − 2.0 mm, lateral ± 1.5 mm, dorsoventral − 1.4 mm from the dura). Glass pipettes used for microinjection were kept in place for 5 min after the injection had been completed to ensure the complete absorption of the viral particles. After recovery in a heated chamber, mice were returned to their home cages. Behavioral tests were performed at 8 weeks after virus injection. Mice that had incorrect injection sites were excluded from the behavioral data analysis.

Behavioral testing

Mouse behaviors were recorded using video tracking software SMART 3.0 (Panlab). For contextual fear conditioning, the sound-attenuating apparatus was equipped with a stainless steel foot-shock grid and interchangeable walls to allow context changes. All mice were habituated in the conditioning chamber for 3 min to reduce basal freezing levels. On the conditioning day, 24 hrs after habituation, all subjects were placed back into the same chamber. Mice were allowed to explore the chamber for 3 min, and then, they received 3 electric foot-shocks (0.5 mA, 2 sec) at intervals of 1 min as an unconditioned stimulus (US). After the last shock, mice were removed from the chamber. On the contextual test day, all subjects were put into the same chamber and were exposed to the same context without exposure to the adverse stimulus. The duration of freezing behaviors was automatically calculated for 5 min (freezing criterion: 1 sec).

Transmission electron microscopy

Four-month-old male WT and 3xTg-AD mice transduced with lentivirus expressing either control or RAPGEF2-shRNA (n = 3 per group) were perfused with 2% PFA and 2.5% glutaraldehyde in 0.15 M cacodylate buffer (pH 7.4). Using a vibratome, 150-μm coronal sections were obtained, and the hippocampal CA1 stratum radiatum was dissected out. Tissue blocks were prepared using standard procedures for TEM as described previously [33]. Briefly, tissue was postfixed in 2% OsO4 for 1 hr, en bloc

stained with 1% uranyl acetate, dehydrated, and then embedded in Epon 812 resin (EMS). Seventy-nanometer-thick sections were collected on 200-mesh grids and stained with uranyl acetate followed by lead citrate. For each animal, 30 images were recorded on a Tecnai F20 TEM (FEI) (2500 × magnification, 120 kV). The counting frame (6 × 6 μm^2) was placed on each image, and synapses with a clear PSD and presynaptic vesicles were identified. Synapses were classified into either asymmetric (excitatory) or symmetric (inhibitory) types based on their distinct PSD shapes. All analyses were performed blinded to the experimental conditions.

Statistical analysis

All data represent the mean ± SEM of at least three independent experiments, unless otherwise indicated. For two-sample comparisons, two-tailed unpaired Student's t tests were used. For three-sample comparisons, one-way ANOVA and Tukey's multiple-comparisons test were used.

For comparing cumulative distributions, the Kolmogorov–Smirnov (KS) test was used. Statistically significant differences were determined at $p < 0.05$.

Results

RAPGEF2 is upregulated in human and mouse AD brains

RAPGEF2 expression is highly enriched in the hippocampus [22, 34], which is critical for learning and memory and is especially vulnerable to damage in the early stages of AD. To test whether RAPGEF2 is involved in the pathophysiological mechanisms of AD, we examined the expression levels of RAPGEF2 in the lysates of postmortem human AD hippocampal tissue using western blot analysis (Fig. 1). Compared to non-AD controls, RAPGEF2 levels were upregulated in hippocampal lysates from AD patients (Fig. 1a). The quantitation of RAPGEF2 band intensity normalized to housekeeping GAPDH signals displayed a significant increase in the levels of RAPGEF2 in human AD brains by approximately two-fold (Fig. 1b).

To identify whether RAPGEF2 levels are also altered in transgenic mouse models of AD, we performed western blot analysis of the cortical and hippocampal lysates obtained from 3- and 12-month-old 3xTg-AD mice (Fig. 2a-c; Additional file 1), one of the most well-characterized and widely used AD mouse models that overexpresses three mutations associated with familial AD [APP Swedish, microtubule-associated protein tau (MAPT) P301L, and presenilin-1 (PSEN1) M146V] [6]. Neuropathological phenotypes of this model include extracellular Aβ deposits in the frontal cortex by 6 months and neurofibrillary tangles in the hippocampus by 12 months and then later in the cortex [6, 35]. Hippocampus-dependent synaptic and cognitive deficits are observed at 4–6 months of age [35, 36]. Intriguingly, we found a significant increase in the RAPGEF2 levels in 3-month-old 3xTg-AD mouse brains (Fig. 2a-c). RAPGEF2 levels in 12-month-old mutants showed an increasing trend but were statistically nonsignificant (Additional file 1). These observations indicate that the upregulation of RAPGEF2 before the onset of synaptic and cognitive impairments may contribute to early pathogenic mechanisms of AD.

To corroborate these results and to narrow down the genetic mutations responsible for the upregulation of RAPGEF2, we next employed two additional AD mouse models expressing mutations associated with familial AD (5xFAD for APP and PSEN1 mutations; rTg4510 for MAPT P301L) [37, 38]. In 5xFAD mice, intraneuronal Aβ was observed in cortical pyramidal neurons at 1.5 months of age, and extracellular amyloid plaques were detected in the hippocampus and cortex of 2-month-old animals [39]. Evidence of synaptic deficits in 5xFAD mice was obtained at 2–3 months using electrophysiology [40]. Furthermore, the loss of synapses and some cognitive impairments were observed at 3–6 months in 5xFAD mice [41]. However, rTg4510 mice expressing human P301L mutant tau in the forebrain by the CaMKIIα (calcium/calmodulin-dependent protein kinase type II subunit alpha) promoter develop progressive neurofibrillary tangles by 4-5.5 months, impaired CA1 long-term potentiation at 4.5 months, a loss of hippocampal and cortical neurons by > 5.5 months, and behavioral impairments between 2 and 6 months of age [37, 42–44].

Again, western blot analysis revealed significantly increased RAPGEF2 levels in the cortical lysates of 1.5-month 5xFAD mice (Fig. 2d and e). In contrast, there were no differences in the RAPGEF2 levels in the cortex and hippocampus between 2.5 and 5.5 months in rTg4510 and age-matched control animals (Additional file 2). These data indicate that amyloid, but not tau, pathology contributes to enhanced RAPGEF2 expression in 3xTg-AD brains. Taken together, these results demonstrate that RAPGEF2 levels are commonly upregulated in sporadic human AD and APP transgenic mouse brains and suggest that RAPGEF2 may participate in the early pathological mechanisms of AD.

Oligomeric Aβ induces the upregulation of RAPGEF2

Because amyloid plaques and neurofibrillary tangles have not yet manifested in 3-month-old 3xTG-AD mice nor in 1.5-month-old 5xFAD mutants [6, 38], we speculated that either full-length APP or Aβ oligomers may trigger the upregulation of RAPGEF2 expression. Indeed, dot blot analysis investigating the amount of Aβ oligomers using 6E10 (anti-Aβ, also recognizes APP) and A11 (anti-amyloidogenic protein oligomer) antibodies [45] exhibited increased levels of oligomeric species in the cortical lysates of 1.5-month-old 5xFAD mice (Additional file 3a).

To further provide direct evidence, we next generated Aβ oligomers by incubating the Aβ peptide for 24 hrs (Fig. 3a) and then examined the RAPGEF2 levels in cultured neurons treated with Aβ oligomers (1 μM) for 6 hrs. Both western blotting and immunofluorescence staining confirmed heightened levels of endogenous RAPGEF2 in cortical and hippocampal neurons following Aβ oligomer treatment (Fig. 3b-e). In contrast, we observed an inverse relationship between the amount of the full-length APP (APP770) and RAPGEF2 levels in heterologous cells (Additional file 3b), supporting the role of oligomeric Aβ rather than full-length APP in the upregulation of RAPGEF2. Thus, our results indicate that Aβ oligomers are sufficient to elevate RAPGEF2 expression in neurons.

Oligomeric Aβ-mediated upregulation of RAPGEF2 activates the Rap2-JNK pathway

The small GTPases Rap1 and Rap2 are well-established downstream effectors of RAPGEF2 [22, 23]. At neuronal synapses, Rap1 and Rap2 are involved in different forms of synaptic plasticity through the regulation of specific signaling pathways [28]. To test whether Aβ oligomer-induced RAPGEF2 may selectively activate its downstream signaling targets, active Rap pull-down assays were performed from cortical lysates of 2.5-month-old 3xTg-AD mice using RalGDS-RBD agarose beads that pull down active GTP-bound Rap.

We found a significant increase in the levels of active Rap2 in 3xTg-AD mice compared to those in wild-type (WT) animals, while active Rap1 levels were nonsignificant between genotypes (Fig. 4a-d). Because JNK is a known downstream effector of Rap2 [27, 28], we next investigated the phosphorylation status of JNK in 3xTg-AD and 5xFAD mice. As expected, JNK phosphorylation levels were significantly higher in the cortex of 2.5-month-old 3xTg-AD and 1.5-month-old 5xFAD mice than in WT controls (Fig. 4e and g; Additional files 4a and b). In contrast, the phosphorylation and total levels of p38 MAPK (mitogen-activated protein kinase), a downstream target of Rap1, did not change in 3xTg-AD mice compared to controls (Fig. 4f and h). Additionally, the decreased phosphorylation levels of ERK were observed in 1.5-month-old 5xFAD mice, in agreement with a previous finding showing that active Rap2 also reduced ERK (extracellular signal-regulated kinases) signaling [27] (Additional file 4c and d). Collectively, these findings indicate that the Aβ oligomer-mediated stimulation of RAPGEF2 expression preferentially activates the Rap2-JNK, but not Rap1-p38, signaling pathway.

Silencing of RAPGEF2 prevents Aβ oligomer-induced spine loss

Aβ oligomer activates JNK before synaptopathy in hippocampal neurons, and the inhibition of JNK blocks spine loss induced by Aβ oligomer [46, 47]. Moreover, transgenic mice expressing constitutively active Rap2 had shorter and fewer dendritic spines in the hippocampus [27]. Thus, we reasoned that the Aβ oligomer-mediated upregulation of RAPGEF2 may participate in the early synaptic pathology of AD.

To confirm that the Aβ oligomer induces synaptopathy in our culture system, we initially examined changes in spine number and morphology in green fluorescent protein (GFP)-expressing hippocampal neurons following Aβ oligomer treatment for 10 hrs. As expected, neurons treated with Aβ oligomers had fewer and smaller spines than control neurons (Additional file 5a-d). Cumulative distribution plots also showed significant reductions in spine length and head size (Additional file 5e and F; Additional file 6).

To test whether silencing RAPGEF2 could prevent Aβ oligomer-induced synaptopathy, we used the RNA interference-mediated knockdown of RAPGEF2 (validated in Additional file 7a and b). Hippocampal neurons were transfected with RAPGEF2-shRNA for 3 days. Upon treatment with Aβ oligomers, we found that neurons expressing RAPGEF2-shRNA had significantly higher spine densities than neurons transfected with the scrambled shRNA control (Fig. 5a and b). However, there were no differences in spine length or head size between groups (Fig. 5c-f and Additional file 6), suggesting that Aβ oligomers involve

multiple signaling pathways in parallel to regulate distinct aspects of synaptic pathology. These results demonstrate that RAPGEF2 knockdown blocks Aβ oligomer-mediated spine loss in hippocampal neurons.

RAPGEF2 knockdown alleviates synaptic and cognitive deficits in the AD hippocampus

We then examined whether the in vivo silencing of RAPGEF2 in the hippocampus could prevent synaptic and cognitive impairments in 3xTg-AD mice. Lentiviral particles expressing RAPGEF2-shRNA were bilaterally delivered to hippocampal CA1 regions of 2-month-old 3xTg-AD mice using stereotaxic surgery (Fig. 6a and b, validated in Additional file 7c-f). At 8 weeks after viral injection, mice were subjected to a hippocampus-dependent contextual fear conditioning test [48, 49]. We observed a significant deficit in freezing behavior in relatively young 4-month-old 3xTg-AD mice compared to matched WT animals (Fig. 6c). More importantly, the knockdown of endogenous RAPGEF2 expression successfully blocked the impairment of context-dependent freezing behavior in 3xTg-AD mice (Fig. 6d), implying that the modulation of RAPGEF2 expression prior to synaptic dysfunction is sufficient to retain long-term fear memory in 3xTg-AD mice.

Finally, we examined whether RAPGEF2 knockdown-mediated fear memory retention in 3xTg-AD mice could be due to synaptic preservation in the hippocampal CA1 area. Transmission electron microscopy revealed that the density of excitatory (asymmetric) synapses, but not inhibitory (symmetric) synapses, was significantly decreased in the CA1 stratum radiatum of 3xTg-AD mice compared to WT animals (Fig. 7a-c). In contrast, the knockdown of RAPAGEF2 in 3xTg-AD mice blocked the reduction in excitatory synaptic density (Fig. 7b and c). Again, the number of inhibitory synapses was not affected by the modulation of RAPGEF2 expression (Fig. 7b and c). These results demonstrate that the loss of RAPGEF2 protein halts the Aβ oligomer-mediated reduction in excitatory synapses in vivo without altering inhibitory synapses. Collectively, our data suggest that early intervention regarding RAPGEF2 expression could prevent Aβ oligomer-mediated synaptic and behavioral dysfunction in the AD hippocampus.

Discussion

The accumulation of soluble Aβ from the sequential proteolytic processing of APP and the hyperphosphorylation of tau is a primary hallmark of AD pathogenesis [4, 50]. In this study, we discovered that RAPGEF2 acts as a novel signaling component involved in Aβ oligomer-mediated synaptic and cognitive impairments in AD. Using multiple AD mouse models and postmortem human AD hippocampal tissue, our results indicate that the Aβ oligomer triggers the upregulation of RAPGEF2 levels in AD brains. Increased RAPGEF2 expression induces the loss of synapses via the activation of the Rap2-JNK pathway. Furthermore, the in vivo knockdown of endogenous RAPGEF2 prevents oligomeric Aβ-induced synaptic and cognitive dysfunction. This scenario showing the involvement of RAPGEF2 in the early synaptopathy of AD is summarized in Fig. 8.

One of the best-characterized familial AD models is the 3xTg-AD mouse model, which develops Aβ deposits prior to tangle formation, consistent with the amyloid cascade hypothesis [6]. Interestingly, we observed heightened levels of RAPGEF2 in 3xTg-AD mice at 3 months of age before the onset of synaptic and cognitive deficits (Fig. 2). An analogous result was found in 1.5-month-old 5xFAD mice expressing APP and PSEN1 mutations (Fig. 2) but not in rTg4510 tau mutants at 2.5 and 5.5 months of age (Additional file 2). These results indicate that either full-length APP or its proteolytic product Aβ augments RAPGEF2 expression in early AD brains, suggesting the potentially causative role of RAPGEF2 in subsequent synaptic and cognitive disturbances. Our results revealed that the Aβ oligomer, rather than full-length APP, induces the upregulation of RAPGEF2 levels (Fig. 3, Additional file 2, and Additional file 3). Furthermore, we provided direct evidence that oligomeric Aβ treatment stimulated RAPGEF2 expression in cultured hippocampal neurons (Fig. 3).

Importantly, augmented RAPGEF2 levels were also identified in the postmortem human AD hippocampus (Fig. 1). Because most cases of AD are sporadic (late-onset) and ~ 5% of cases are genetic (early-onset) in origin [51], we assume that the increased RAPGEF2 levels in the human AD hippocampus may reflect the relatively slow and gradual increase in Aβ oligomers in sporadic AD compared to familiar AD. Although it is unclear when RAPGEF2 expression begins to be stimulated in human AD patients, our data show that RAPGEF2 levels are commonly induced in the brains of early- and late-onset AD brains.

Rap1 and Rap2, the downstream effectors of RAPGEF2, are members of the Ras family of small GTPases [22]. Rap1 and Rap2 share close to 60% sequence homology [52], but they seem to exert distinct functions by activating different signaling pathways. For instance, Rap1 and Rap2 regulate the synaptic removal of AMPA-type glutamate receptors via the activation of p38 MAPK during long-term depression and JNK in synaptic depotentiation, respectively [20, 26, 28]. Furthermore, the activation of Rap2 causes the loss of excitatory synapses, while Rap1 has no effects on axonal or dendritic morphology in spiny neurons [21]. In line with these findings, our data show that the Aβ oligomer-mediated stimulation of RAPGEF2 expression selectively activates Rap2-JNK, rather than Rap1-p38 MAPK (Fig. 4), suggesting the distinct roles of Rap proteins in the pathogenetic mechanisms of AD.

The activation of JNK, a downstream target of Rap2, has been reported in human AD brains [53]. Our results also revealed that phosphorylation levels of JNK are significantly higher in cortical lysates from 3xTg-AD and 5xFAD mice during the same period of RAPGEF2 upregulation (Fig. 4 and Additional file 4), which is consistent with the Aβ-mediated activation of the JNK pathway in cultured cortical neurons [46, 54]. Conversely, JNK phosphorylates APP at the Thr688 residue and facilitates Aβ aggregation [55, 56], and the inhibition of JNK reduces soluble Aβ oligomers [57]. Thus, it is likely that Aβ and JNK could create a reciprocal activation circuit that further exacerbates Aβ pathology.

What are the upstream molecules that trigger the upregulation of RAPGEF2? Polo-like kinase 2 (Plk2) could be one of the candidates involved in Aβ-mediated synaptopathy, as Plk2 has been shown to promote RAPGEF2 activity in the hippocampus [25]. In support of this idea, increased levels of Plk2 were also observed in the APP-SwD1 AD mouse brain and in the human AD brain [58]. Furthermore, the

pharmacological inhibition of Plk2 function ameliorates synapse loss and memory decline in an AD mouse model [58]. Thus, these findings suggest that Plk2 may act as an upstream regulator in RAPGEF2-mediated synaptic dysfunction and cognitive deficits. Further studies are warranted to identify additional upstream signaling molecules that trigger the upregulation of RAPGEF2.

Previous studies have reported that constitutively active Rap2 reduces the number and length of dendritic spines in CA1 hippocampal neurons [27], and JNK inhibition rescues Aβ oligomer-mediated spine loss [46]. Thus, it has been speculated that the Aβ oligomer-mediated upregulation of RAPGEF2 levels may induce changes in the number and morphology of dendritic spines by activating the Rap2-JNK signaling cascade. We found that the knockdown of RAPGEF2 restored the Aβ oligomer-mediated loss of dendritic spines but not the length and head size of spines (Fig. 5). These findings indicate that Aβ oligomers may induce multiple signaling pathways that act in parallel to affect distinct morphological aspects of dendritic spines. Indeed, a recent study showed that the Pyk2-Graf1-RhoA pathway plays a role in Aβ-mediated dendritic spinopathy [59].

To our surprise, in vivo silencing of RAPGEF2 in the hippocampal CA1 area was sufficient to preserve contextual fear memory retention (Fig. 6), which requires the intact function of the dorsal hippocampus [60]. Notably, electron microscopy analysis revealed that RAPGEF2 knockdown was sufficient to block the reduction in excitatory synapses in the hippocampal CA1 stratum radiatum of 3xTG-AD mice (Fig. 7).

In summary, our results demonstrate that RAPGEF2 mediates Aβ oligomer-induced synaptic and cognitive deficits in the AD hippocampus. Therefore, early intervention regarding RAPGEF2 expression might be a potential therapeutic option to help mitigate Aβ oligomer-induced synaptic and behavioral impairments in AD.

Conclusions

This study defines a novel role of RAPGEF2 as a molecular link between oligomeric Aβ and synaptic degeneration in AD. The authors show that RAPGEF2 levels were upregulated in the postmortem AD hippocampus and in AD mouse models, generating high levels of Aβ oligomers. This Aβ oligomer-mediated stimulation of RAPGEF2 expression reduces spine numbers via the activation of its downstream signaling targets Rap2 and JNK. Notably, silencing RAPGEF2 in the AD hippocampus blocks Aβ oligomer-induced synapse loss and cognitive dysfunction. Collectively, this study proposes that early intervention regarding RAPGEF2 expression may provide a potential option to help prevent early synaptic and cognitive impairments in AD.

List Of Abbreviations

AD, Alzheimer’s disease; Aβ, amyloid-β; WT, wild-type; TG, transgenic; RBD, Ras-binding domain; APP, amyloid precursor protein; MAPT, microtubule-associated protein tau; PSEN1, presenilin-1; CaMKIIα, calcium/calmodulin-dependent protein kinase type II subunit alpha; MAPK, mitogen-activated protein

kinase; JNK, c-Jun N-terminal kinases; ERK, extracellular signal-regulated kinases; GFP, green fluorescent protein; PSD, postsynaptic density.

Declarations

Ethics approval

All animal experiments were carried out in compliance with the Guide for Care and Use of Laboratory Animals of the National Institutes of Health and were approved by the Institutional Animal Care and Use Committee of Korea Brain Research Institute (IACUC 17-00017, 17-00018, 18-00016, and 18-00026). Human hippocampal tissue samples used in this study were obtained from the Netherlands Brain Bank (Project #1009, Amsterdam, Netherland). Experiments using human tissue were approved by the Institutional Review Board at Korea Brain Research Institute (201610-BR-004-01).

Consent for publication

Not applicable.

Availability of data and materials

All data generated or analyzed during this study are included in this published article and its supplementary information files.

Competing interests

The authors declare no competing financial interests.

Funding

This work was supported by the KBRI basic research program (19-BR-01-01 to K.J.L.) and grants from the Korean NRF funded by the Ministry of Education (NRF-2014R1A1A2058740 to K.J.L.) and the Ministry of Science and ICT (NRF-2017M3C7A1048086 to K.J.L.), and the Korea Health Technology R&D Project of the Ministry for Health and Welfare (HI14C1135 to K.J.L.).

Authors' contributions

K.J.L. designed the experiments, wrote the manuscript, and supervised the project. Y.-N.J., H.J., J.E.N., and K.-A.C. performed biochemical, imaging, and behavioral experiments and analyzed the data. G.H.K. performed transmission electron microscopy and analyzed the data. Y.-N.J. wrote the initial draft of the manuscript. All authors read and approved the final manuscript.

Acknowledgements

The authors thank the members of the Brain Research Core Facilities in KBRI for their assistance with the confocal and electron microscopic experiments.

References

1. Selkoe DJ. Alzheimer's disease is a synaptic failure. Science. 2002;298(5594):789-91.
2. Sivanesan S, Tan A, Rajadas J. Pathogenesis of Abeta oligomers in synaptic failure. Curr Alzheimer Res. 2013;10(3):316-23.
3. Selkoe DJ. Soluble oligomers of the amyloid beta-protein impair synaptic plasticity and behavior. Behav Brain Res. 2008;192(1):106-13.
4. Cavallucci V, D'Amelio M, Cecconi F. Abeta toxicity in Alzheimer's disease. Mol Neurobiol. 2012;45(2):366-78.
5. DeKosky ST, Scheff SW. Synapse loss in frontal cortex biopsies in Alzheimer's disease: correlation with cognitive severity. Ann Neurol. 1990;27(5):457-64.
6. Oddo S, Caccamo A, Shepherd JD, Murphy MP, Golde TE, Kayed R, et al. Triple-transgenic model of Alzheimer's disease with plaques and tangles: intracellular Abeta and synaptic dysfunction. Neuron. 2003;39(3):409-21.
7. Dickson DW, Crystal HA, Bevona C, Honer W, Vincent I, Davies P. Correlations of synaptic and pathological markers with cognition of the elderly. Neurobiol Aging. 1995;16(3):285-98; discussion 98-304.
8. Masliah E, Mallory M, Alford M, DeTeresa R, Hansen LA, McKeel DW, Jr., et al. Altered expression of synaptic proteins occurs early during progression of Alzheimer's disease. Neurology. 2001;56(1):127-9.
9. Kuo YM, Emmerling MR, Vigo-Pelfrey C, Kasunic TC, Kirkpatrick JB, Murdoch GH, et al. Water-soluble Abeta (N-40, N-42) oligomers in normal and Alzheimer disease brains. J Biol Chem. 1996;271(8):4077-81.
10. Gong Y, Chang L, Viola KL, Lacor PN, Lambert MP, Finch CE, et al. Alzheimer's disease-affected brain: presence of oligomeric A beta ligands (ADDLs) suggests a molecular basis for reversible memory loss. Proc Natl Acad Sci U S A. 2003;100(18):10417-22.
11. Klyubin I, Walsh DM, Cullen WK, Fadeeva JV, Anwyl R, Selkoe DJ, et al. Soluble Arctic amyloid beta protein inhibits hippocampal long-term potentiation in vivo. Eur J Neurosci. 2004;19(10):2839-46.
12. Wang Q, Walsh DM, Rowan MJ, Selkoe DJ, Anwyl R. Block of long-term potentiation by naturally secreted and synthetic amyloid beta-peptide in hippocampal slices is mediated via activation of the kinases c-Jun N-terminal kinase, cyclin-dependent kinase 5, and p38 mitogen-activated protein kinase as well as metabotropic glutamate receptor type 5. J Neurosci. 2004;24(13):3370-8.
13. Harris KM, Kater SB. Dendritic spines: cellular specializations imparting both stability and flexibility to synaptic function. Annu Rev Neurosci. 1994;17:341-71.
14. Kamenetz F, Tomita T, Hsieh H, Seabrook G, Borchelt D, Iwatsubo T, et al. APP processing and synaptic function. Neuron. 2003;37(6):925-37.

15. Cirrito JR, Yamada KA, Finn MB, Sloviter RS, Bales KR, May PC, et al. Synaptic activity regulates interstitial fluid amyloid-beta levels in vivo. Neuron. 2005;48(6):913-22.
16. Lee Y, Lee JS, Lee KJ, Turner RS, Hoe HS, Pak DTS. Polo-like kinase 2 phosphorylation of amyloid precursor protein regulates activity-dependent amyloidogenic processing. Neuropharmacology. 2017;117:387-400.
17. Chong YH, Shin YJ, Lee EO, Kayed R, Glabe CG, Tenner AJ. ERK1/2 activation mediates Abeta oligomer-induced neurotoxicity via caspase-3 activation and tau cleavage in rat organotypic hippocampal slice cultures. J Biol Chem. 2006;281(29):20315-25.
18. Knox AL, Brown NH. Rap1 GTPase regulation of adherens junction positioning and cell adhesion. Science. 2002;295(5558):1285-8.
19. Franco SJ, Martinez-Garay I, Gil-Sanz C, Harkins-Perry SR, Muller U. Reelin regulates cadherin function via Dab1/Rap1 to control neuronal migration and lamination in the neocortex. Neuron. 2011;69(3):482-97.
20. Zhu JJ, Qin Y, Zhao M, Van Aelst L, Malinow R. Ras and Rap control AMPA receptor trafficking during synaptic plasticity. Cell. 2002;110(4):443-55.
21. Fu Z, Lee SH, Simonetta A, Hansen J, Sheng M, Pak DT. Differential roles of Rap1 and Rap2 small GTPases in neurite retraction and synapse elimination in hippocampal spiny neurons. J Neurochem. 2007;100(1):118-31.
22. de Rooij J, Boenink NM, van Triest M, Cool RH, Wittinghofer A, Bos JL. PDZ-GEF1, a guanine nucleotide exchange factor specific for Rap1 and Rap2. J Biol Chem. 1999;274(53):38125-30.
23. Liao Y, Kariya K, Hu CD, Shibatohge M, Goshima M, Okada T, et al. RA-GEF, a novel Rap1A guanine nucleotide exchange factor containing a Ras/Rap1A-associating domain, is conserved between nematode and humans. J Biol Chem. 1999;274(53):37815-20.
24. Ohtsuka T, Hata Y, Ide N, Yasuda T, Inoue E, Inoue T, et al. nRap GEP: a novel neural GDP/GTP exchange protein for rap1 small G protein that interacts with synaptic scaffolding molecule (S-SCAM). Biochem Biophys Res Commun. 1999;265(1):38-44.
25. Lee KJ, Lee Y, Rozeboom A, Lee JY, Udagawa N, Hoe HS, et al. Requirement for Neuron. 2011;69(5):957-73.
26. Zhu Y, Pak D, Qin Y, McCormack SG, Kim MJ, Baumgart JP, et al. Rap2-JNK r removes synaptic AMPA receptors during depotentiation. Neuron. 2005;46(6):905-16.
27. Ryu J, Futai K, Feliu M, Weinberg R, Sheng M. Constitutively active Rap2 transgenic mice display fewer dendritic spines, reduced extracellular signal-regulated kinase signaling, enhanced long-term depression, and impaired spatial learning and fear extinction. J Neurosci. 2008;28(33):8178-88.
28. Zhang L, Zhang P, Wang G, Zhang H, Zhang Y, Yu Y, et al. Ras and Rap Signal Bidirectional Synaptic Plasticity via Distinct Subcellular Microdomains. Neuron. 2018;98(4):783-800 e4.
29. Ishiura H, Doi K, Mitsui J, Yoshimura J, Matsukawa MK, Fujiyama A, et al. Expansions of intronic TTTCA and TTTTA repeats in benign adult familial myoclonic epilepsy. Nat Genet. 2018;50(4):581-90.

30. Minkeviciene R, Rheims S, Dobszay MB, Zilberter M, Hartikainen J, Fulop L, et al. Amyloid beta-induced neuronal hyperexcitability triggers progressive epilepsy. J Neurosci. 2009;29(11):3453-62.
31. Born HA, Kim JY, Savjani RR, Das P, Dabaghian YA, Guo Q, et al. Genetic suppression of transgenic APP rescues Hypersynchronous network activity in a mouse model of Alzeimer's disease. J Neurosci. 2014;34(11):3826-40.
32. Amatniek JC, Hauser WA, DelCastillo-Castaneda C, Jacobs DM, Marder K, Bell K, et al. Incidence and predictors of seizures in patients with Alzheimer's disease. Epilepsia. 2006;47(5):867-72.
33. Lee KJ, Park IS, Kim H, Greenough WT, Pak DT, Rhyu IJ. Motor skill training induces coordinated strengthening and weakening between neighboring synapses. J Neurosci. 2013;33(23):9794-9.
34. Hisata S, Sakisaka T, Baba T, Yamada T, Aoki K, Matsuda M, et al. Rap1-PDZ-GEF1 interacts with a neurotrophin receptor at late endosomes, leading to sustained activation of Rap1 and ERK and neurite outgrowth. J Cell Biol. 2007;178(5):843-60.
35. Billings LM, Oddo S, Green KN, McGaugh JL, LaFerla FM. Intraneuronal Abeta causes the onset of early Alzheimer's disease-related cognitive deficits in transgenic mice. Neuron. 2005;45(5):675-88.
36. Stover KR, Campbell MA, Van Winssen CM, Brown RE. Early detection of cognitive deficits in the 3xTg-AD mouse model of Alzheimer's disease. Behav Brain Res. 2015;289:29-38.
37. Ramsden M, Kotilinek L, Forster C, Paulson J, McGowan E, SantaCruz K, et al. Age-dependent neurofibrillary tangle formation, neuron loss, and memory impairment in a mouse model of human tauopathy (P301L). J Neurosci. 2005;25(46):10637-47.
38. Jawhar S, Trawicka A, Jenneckens C, Bayer TA, Wirths O. Motor deficits, neuron loss, and reduced anxiety coinciding with axonal degeneration and intraneuronal Abeta aggregation in the 5XFAD mouse model of Alzheimer's disease. Neurobiol Aging. 2012;33(1):196 e29-40.
39. Richard BC, Kurdakova A, Baches S, Bayer TA, Weggen S, Wirths O. Gene Dosage Dependent Aggravation of the Neurological Phenotype in the 5XFAD Mouse Model of Alzheimer's Disease. J Alzheimers Dis. 2015;45(4):1223-36.
40. Buskila Y, Crowe SE, Ellis-Davies GC. Synaptic deficits in layer 5 neurons precede overt structural decay in 5xFAD mice. Neuroscience. 2013;254:152-9.
41. Crowe SE, Ellis-Davies GC. In vivo characterization of a bigenic fluorescent mouse model of Alzheimer's disease with neurodegeneration. J Comp Neurol. 2013;521(10):2181-94.
42. Helboe L, Egebjerg J, Barkholt P, Volbracht C. Early depletion of CA1 neurons and late neurodegeneration in a mouse tauopathy model. Brain Res. 2017;1665:22-35.
43. Spires TL, Orne JD, SantaCruz K, Pitstick R, Carlson GA, Ashe KH, et al. Region-specific dissociation of neuronal loss and neurofibrillary pathology in a mouse model of tauopathy. Am J Pathol. 2006;168(5):1598-607.
44. Blackmore T, Meftah S, Murray TK, Craig PJ, Blockeel A, Phillips K, et al. Tracking progressive pathological and functional decline in the rTg4510 mouse model of tauopathy. Alzheimers Res Ther. 2017;9(1):77.

45. Kim HY, Kim HV, Jo S, Lee CJ, Choi SY, Kim DJ, et al. EPPS rescues hippocampus-dependent cognitive deficits in APP/PS1 mice by disaggregation of amyloid-beta oligomers and plaques. Nat Commun. 2015;6:8997.
46. Sclip A, Arnaboldi A, Colombo I, Veglianese P, Colombo L, Messa M, et al. Soluble Abeta oligomer-induced synaptopathy: c-Jun N-terminal kinase's role. J Mol Cell Biol. 2013;5(4):277-9.
47. Sclip A, Tozzi A, Abaza A, Cardinetti D, Colombo I, Calabresi P, et al. c-Jun N-terminal kinase has a key role in Alzheimer disease synaptic dysfunction in vivo. Cell Death Dis. 2014;5:e1019.
48. Huckleberry KA, Ferguson LB, Drew MR. Behavioral mechanisms of context fear generalization in mice. Learn Mem. 2016;23(12):703-9.
49. Blaeser F, Sanders MJ, Truong N, Ko S, Wu LJ, Wozniak DF, et al. Long-term memory deficits in Pavlovian fear conditioning in Ca2+/calmodulin kinase kinase alpha-deficient mice. Mol Cell Biol. 2006;26(23):9105-15.
50. Zhang H, Ma Q, Zhang YW, Xu H. Proteolytic processing of Alzheimer's beta-amyloid precursor protein. J Neurochem. 2012;120 Suppl 1:9-21.
51. Bali J, Gheinani AH, Zurbriggen S, Rajendran L. Role of genes linked to sporadic Alzheimer's disease risk in the production of beta-amyloid peptides. Proc Natl Acad Sci U S A. 2012;109(38):15307-11.
52. Ohba Y, Mochizuki N, Matsuo K, Yamashita S, Nakaya M, Hashimoto Y, et al. Rap2 as a slowly responding molecular switch in the Rap1 signaling cascade. Mol Cell Biol. 2000;20(16):6074-83.
53. Zhu X, Raina AK, Rottkamp CA, Aliev G, Perry G, Boux H, et al. Activation and redistribution of c-jun N-terminal kinase/stress activated protein kinase in degenerating neurons in Alzheimer's disease. J Neurochem. 2001;76(2):435-41.
54. Morishima Y, Gotoh Y, Zieg J, Barrett T, Takano H, Flavell R, et al. Beta-amyloid induces neuronal apoptosis via a mechanism that involves the c-Jun N-terminal kinase pathway and the induction of Fas ligand. J Neurosci. 2001;21(19):7551-60.
55. Ahn JH, So SP, Kim NY, Kim HJ, Yoon SY, Kim DH. c-Jun N-terminal Kinase (JNK) induces phosphorylation of amyloid precursor protein (APP) at Thr668, in okadaic acid-induced neurodegeneration. BMB Rep. 2016;49(7):376-81.
56. Muresan Z, Muresan V. c-Jun NH2-terminal kinase-interacting protein-3 facilitates phosphorylation and controls localization of amyloid-beta precursor protein. J Neurosci. 2005;25(15):3741-51.
57. Sclip A, Antoniou X, Colombo A, Camici GG, Pozzi L, Cardinetti D, et al. c-Jun N-terminal kinase regulates soluble Abeta oligomers and cognitive impairment in AD mouse model. J Biol Chem. 2011;286(51):43871-80.
58. Lee JS, Lee Y, Andre EA, Lee KJ, Nguyen T, Feng Y, et al. Inhibition of Polo-like kinase 2 ameliorates pathogenesis in Alzheimer's disease model mice. PLoS One. 2019;14(7):e0219691.
59. Lee S, Salazar SV, Cox TO, Strittmatter SM. Pyk2 Signaling through Graf1 and RhoA GTPase Is Required for Amyloid-beta Oligomer-Triggered Synapse Loss. J Neurosci. 2019;39(10):1910-29.

60. McNish KA, Gewirtz JC, Davis M. Evidence of contextual fear after lesions of the hippocampus: a disruption of freezing but not fear-potentiated startle. J Neurosci. 1997;17(23):9353-60.

Additional Files

Additional file 1.pdf

No change in RAPGEF2 levels in 12-month-old 3xTg-AD mice (related to Fig. 2). **a** and **b,** RAPGEF2 levels were analyzed at 3 months of age in the hippocampus (HPC, in a) and cortex (CTX, in b) of wild-type (WT) and 3xTg-AD mice (TG). **c**, Quantification of RAPGEF2 levels in the HPC and CTX of WT and TG mice. The data are shown as the mean ± SEM (n=4). Two-tailed unpaired Student's *t*-test.

Additional file 2.pdf

No change in RAPGEF2 levels in rTg4510 human tau-mutant mice (related to Fig. 3)**. a**–**d,** RAPGEF2 levels were analyzed in the hippocampus (HPC) and cortex (CTX) of wild-type (WT) and rTg4510 (TG) mice at 2.5 months of age (a and c) and 5.5 months of age (b and d). Levels of total tau and phospho-tau were detected with Tau5 and AT8 antibodies, respectively. **e** and **f,** Quantification of RAPGEF2 levels in the HPC and CTX of WT and TG at 2.5 months of age (e) and 5.5 months of age (f). All data are shown as the mean ± SEM (2.5 months of age, n=6; 5.5 months of age, n=4). Two-tailed unpaired Student's *t*-test.

Additional file 3.pdf

a, Increased levels of Aβ oligomer in the cortex of 1.5-month-old 5xFAD mice (related to Fig. 3)**.** Dot blot assay. Levels of total and oligomeric Aβ were detected with 6E10 and A11 antibodies, respectively (WT, n=2; TG, n=6). **b**, **Reduced RAPGEF2 levels by coexpressing full-length APP (**related to Fig. 3). HA-tagged RAPGEF2 (0.5 μg) was cotransfected with APP770-GFP into COS-7 cells for 24 hrs. RAPGEF2 levels gradually decreased in the presence of APP770-GFP (0, 0.4, 0.6, 0.8 μg).

Additional file 4.pdf

Stimulation of JNK and reduced ERK activity in 1.5-month-old 5xFAD mice (related to Fig. 4)**. a** and **b**, Increased JNK activity in 5xFAD mice at 1.5 months of age (n=5). **c** and **d,** Decreased ERK activity in 5xFAD mice at 1.5 months of age (n=5). All data are shown as the mean ± SEM. ***p<0.001, *p<0.05; two-tailed unpaired Student's *t*-test.

Additional file 5.pdf

Aβ oligomer-mediated reduction in spine density, length, and head size (related Fig. 5)**. a,** Representative GFP fluorescence images of cultured hippocampal neurons. Neurons (DIV 21) were treated with oligomeric Aβ (AβO, 1 μM) for 10 hrs before immunostaining. Bottom, Enlarged images of the data enclosed in rectangles at the top. Scale, 10 μm. **b-d,** Quantification of spine density (b), length (c), and

head size (d) (n=14 neurons per group). **e and f**, Cumulative distribution plots of spine length and head size (n=900~1020 spines; K–S test; see Additional file 6). All data are shown as the mean ± SEM. *p<0.05, **p<0.01, **** p<0.0001; two-tailed unpaired Student's t-test.

Additional file 6.pdf

Table. Kolmogorov–Smirnov (KS) test for spine length and head size (related Fig. 5)**.** To compare cumulative distributions of dendritic spine length and head size, the Kolmogorov–Smirnov (KS) test was used.

Additional file 7.pdf

Knockdown effect of shRNA against endogenous RAPGEF2 (related Fig. 5-7)**. a** and **b,** The florescence intensity of RAPGEF2 was substantially decreased in rat hippocampal neurons transfected with shRAPGEF2 (related Fig. 5). Arrowheads indicate neurons transfected with scrambled shRNA or shRAPGEF2 (n=5 per condition). Scale, 50 μm. **c** and **d**, The florescence intensity of RAPGEF2 was significantly reduced in mouse hippocampal neurons transfected with shRAPGEF2 (related Fig. 6 and 7). Arrowheads indicate neurons transfected with pll3.7 (control) and shRAPGEF2 (n=6). Scale, 50 μm. **e** and **f,** RAPGEF2 levels were markedly decreased by shRAPGEF2 expression (related Fig. 6 and 7)**.** Mouse hippocampal neuronal lysates were used for western blot analysis of RAPGEF2 levels. Lentiviral particles expressing either shRAPGEF2 or a control empty vector (pll3.7) were infected into hippocampal neurons at DIV 7 for 14 days (n=3). All data are shown as the mean ± SEM.. ***p<0.001, **p<0.01, *p<0.05; two-tailed unpaired Student's t-test.

Figures

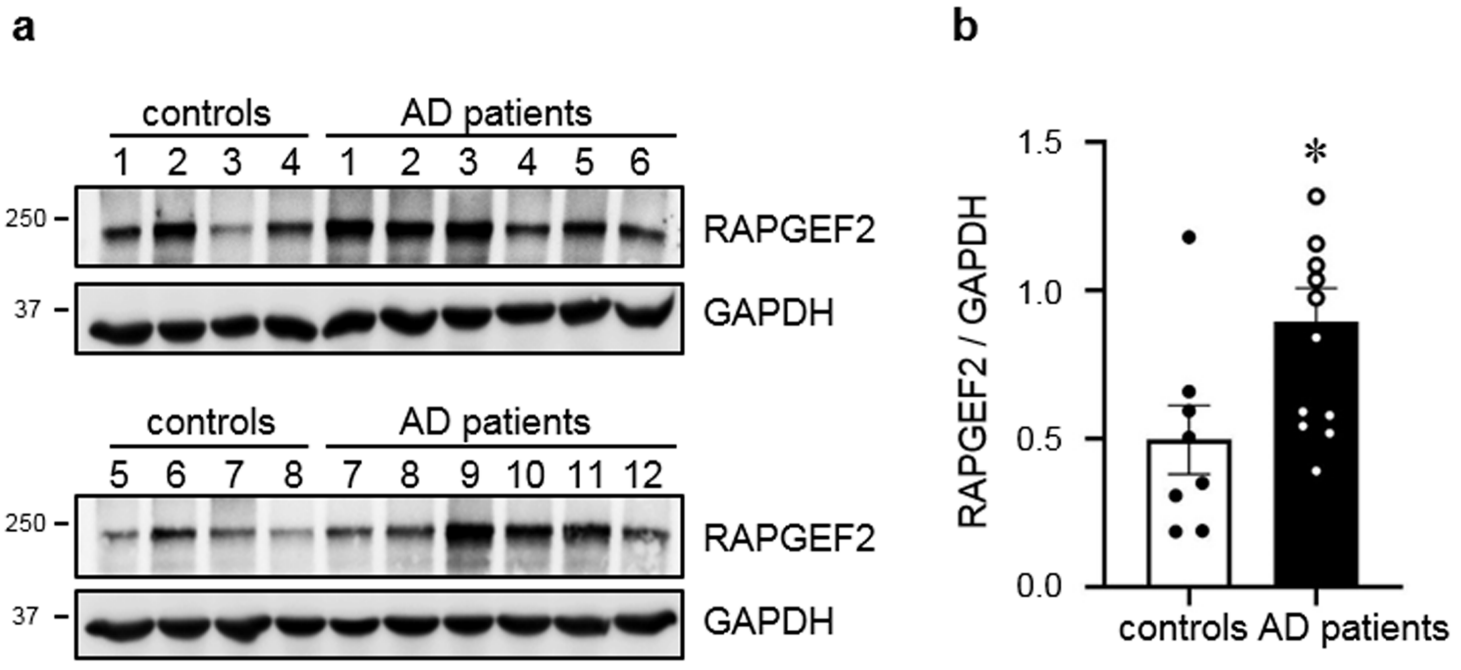

Figure 1

Elevated levels of RAPGEF2 in the postmortem human AD hippocampus. a, Postmortem human hippocampal tissue from nonpatients (control) and AD patients was homogenized and subjected to western blot analysis for the RAPGEF2 levels. b, Quantification of RAPGEF2 expression levels normalized to GAPDH. The data are shown as the mean ± SEM (control, n=8; AD patients, n=12). *p <0.05; two-tailed unpaired Student's t-test.

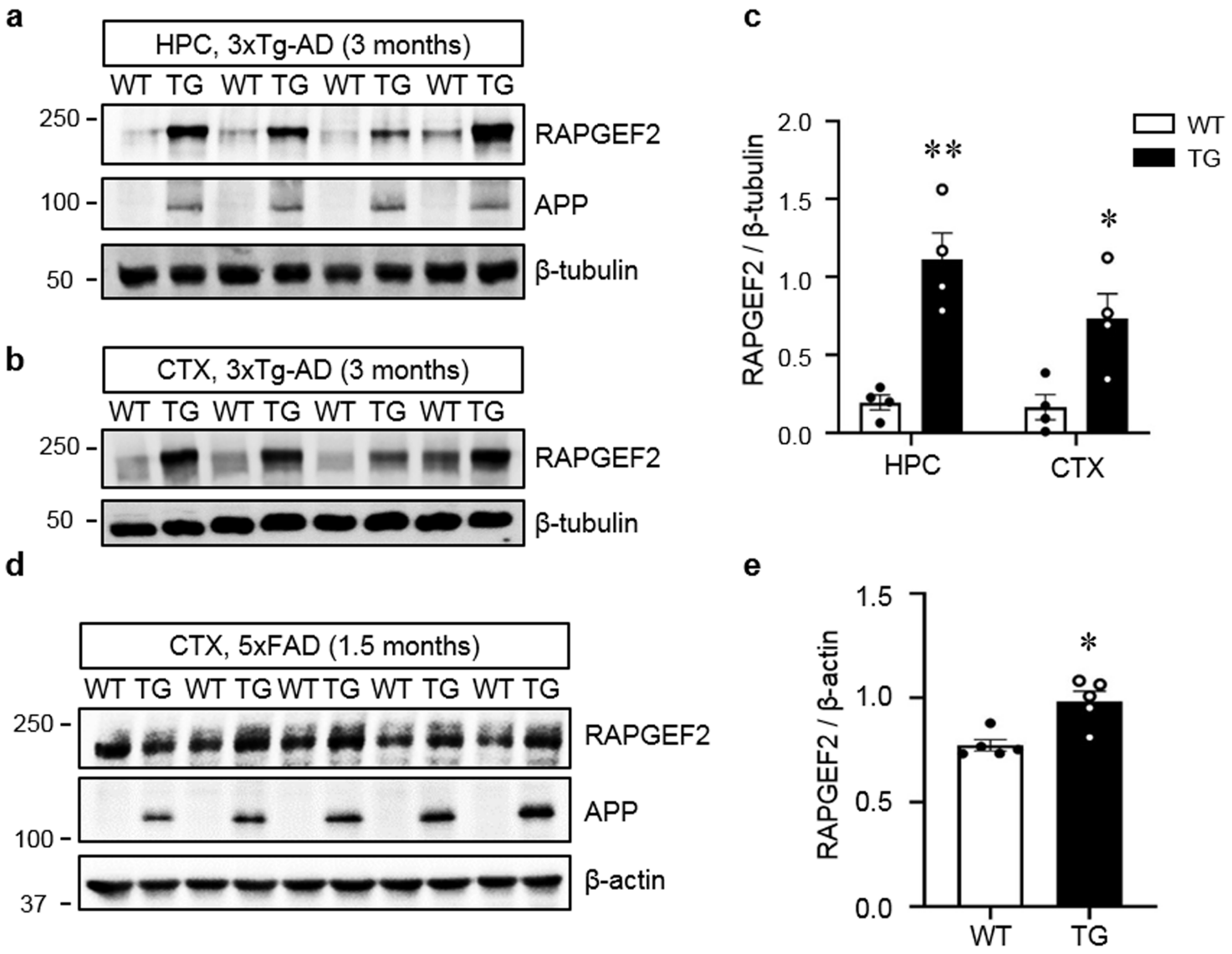

Figure 2

Increased RAPGEF2 levels in 3xTg-AD and 5xFAD mice before the onset of synaptic dysfunction. a and b, RAPGEF2 expression levels were analyzed at 3 months of age in the hippocampus (HPC, in a) and cortex (CTX, in b) of wild-type (WT) and 3xTg-AD mice (TG). c, Quantification of RAPGEF2 levels in the HPC and CTX of 3-month-old WT and TG mice (n=4). d, RAPGEF2 expression levels were analyzed in the cortical lysates of 1.5-month-old WT and 5xFAD (TG) mice. Note that the levels of APP are markedly higher in TG

mice. e, Quantification of RAPGEF2 levels normalized to β-actin (n=5). All data are shown as the mean ± SEM. **p<0.01, *p<0.05; two-tailed unpaired Student's t-test.

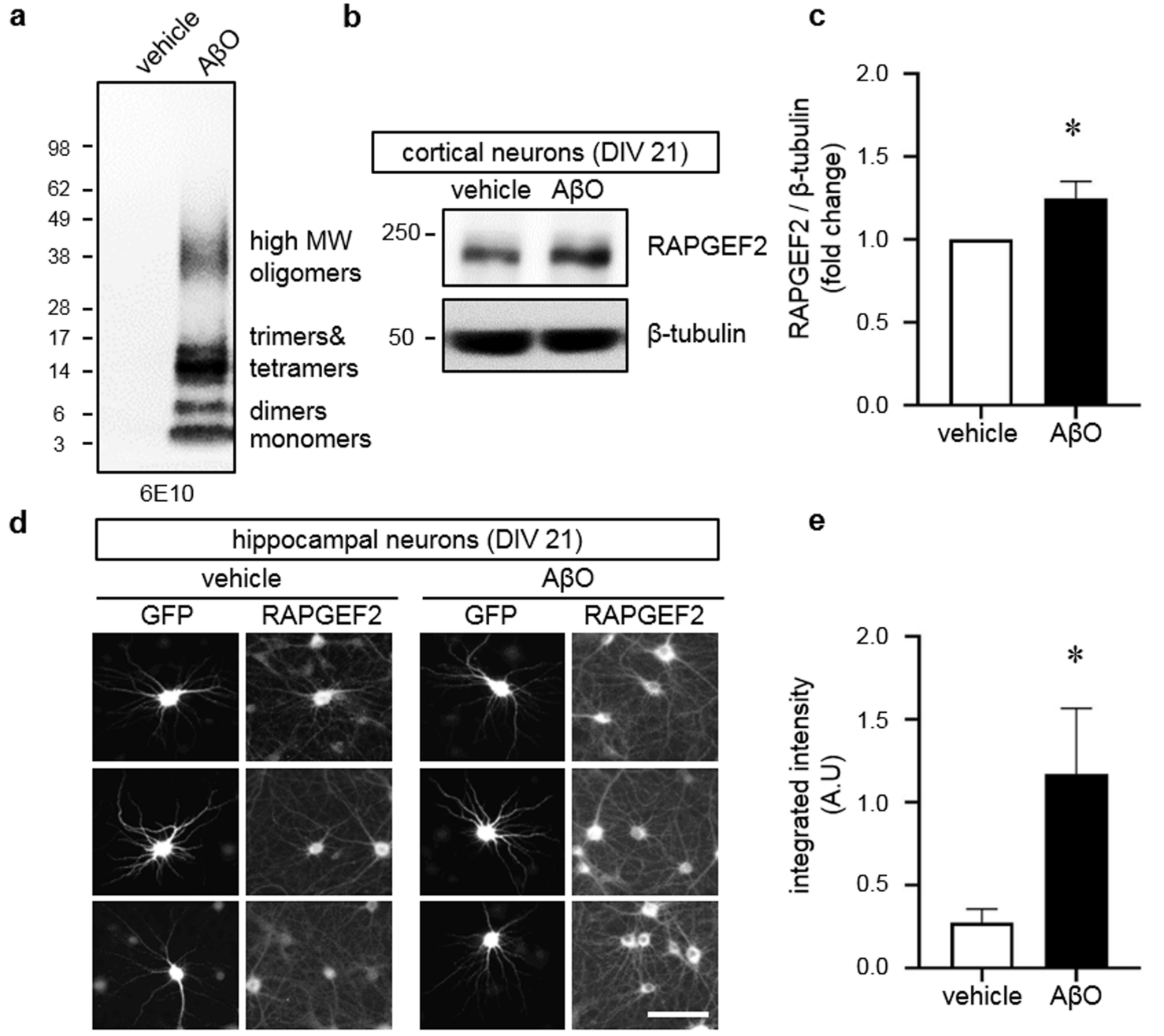

Figure 3

Oligomeric Aβ increases RAPGEF2 levels. a, SDS-PAGE analysis of oligomeric Aβ. Oligomers were separated by western blotting on a 4~12% gradient Bis-Tris gel and immunoblotted with 6E10 antibody. AβO consisted of monomers (~4 kDa), dimers, trimers, tetramers, and high molecular weight (MW) oligomers. No fibrils (>75 kDa) were detected. b, Cultured cortical neurons (DIV 21) treated with vehicle or oligomeric Aβ (AβO, 1 μM) for 6 hrs. Levels of RAPGEF2 were assessed by western blotting using the RAPGEF2 antibody. c, Relative fold change in RAPGEF2 levels (n=7). d, Cultured hippocampal neurons (DIV 21) treated with vehicle or oligomeric Aβ (AβO, 1 μM) for 6 hrs and immunolabeled for GFP and

RAPGEF2. Scale, 100 μm. e, Quantification of the integrated intensity of RAPGEF2 in proximal dendrites (n=12). All data are shown as the mean ± SEM. *p<0.05; two-tailed unpaired Student's t-test.

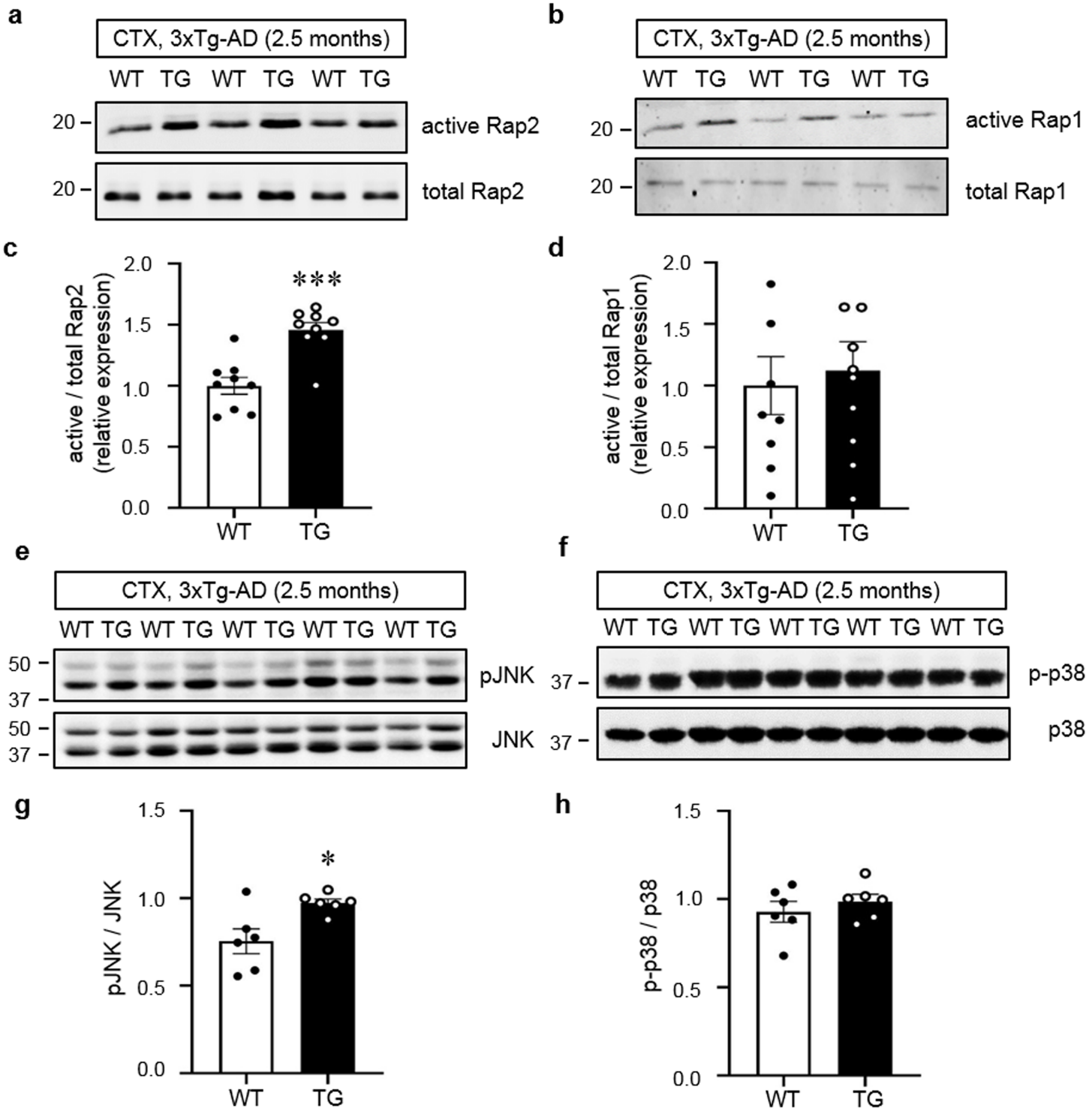

Figure 4

Activation of the small GTPase Rap2-JNK pathway in 3xTg-AD mice. a and b, Cortical lysates from 2.5-month-old wild-type (WT) and 3xTg-AD (TG) mice were incubated with RalGDS-RBD agarose beads, followed by immunoblotting with Rap2 (a) or Rap1 (b) antibodies, respectively. c and d, Quantification of active Rap2 (c) and active Rap1 (d) levels normalized to total Rap2 and Rap1, respectively (n=9). e and f,

Cortical lysates from 2.5-month-old wild-type (WT) and 3xTg-AD (TG) mice were collected and subjected to western blotting. Activation (phosphorylation) of JNK (e) and p38(f) was analyzed by western blotting. g and h, Quantification of pJNK (g, n=7) and p-p38 (h, n=6) levels normalized to total expression. All data are shown as the mean ± SEM. *p<0.05, ***p<0.001; two-tailed unpaired Student's t-test.

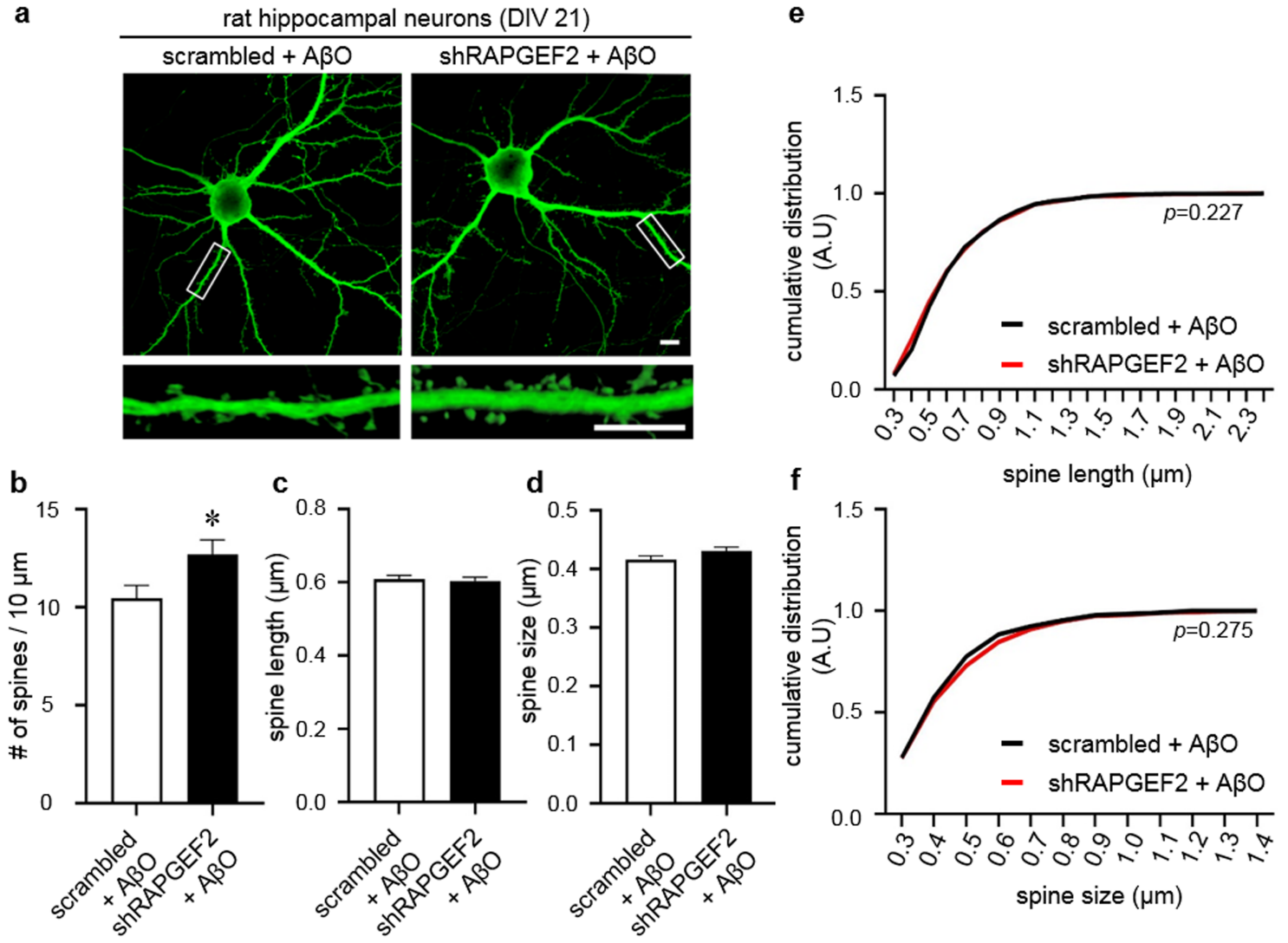

Figure 5

Knockdown of RAPGEF2 prevents the AβO-induced loss of dendritic spines. a, Representative GFP fluorescence images of cultured hippocampal neurons. Neurons at DIV 18 were transfected with either scrambled shRNA or shRAPGEF2 for 3 days and treated with oligomeric Aβ (AβO, 1 μM) for 10 hrs before immunostaining. Bottom, Enlarged images of the data enclosed in rectangles at the top. Scale, 10 μm. b-d, Quantification of spine density (b), spine length (c), and spine head size (d). The data are shown as the mean ± SEM (scrambled, n=21; shRAPGEF2, n=20). *p<0.05; two-tailed unpaired Student's t-test. e and f, Cumulative distribution plots of spine length and spine head size (n=649~768 spines, K–S test; see also Additional file 6).

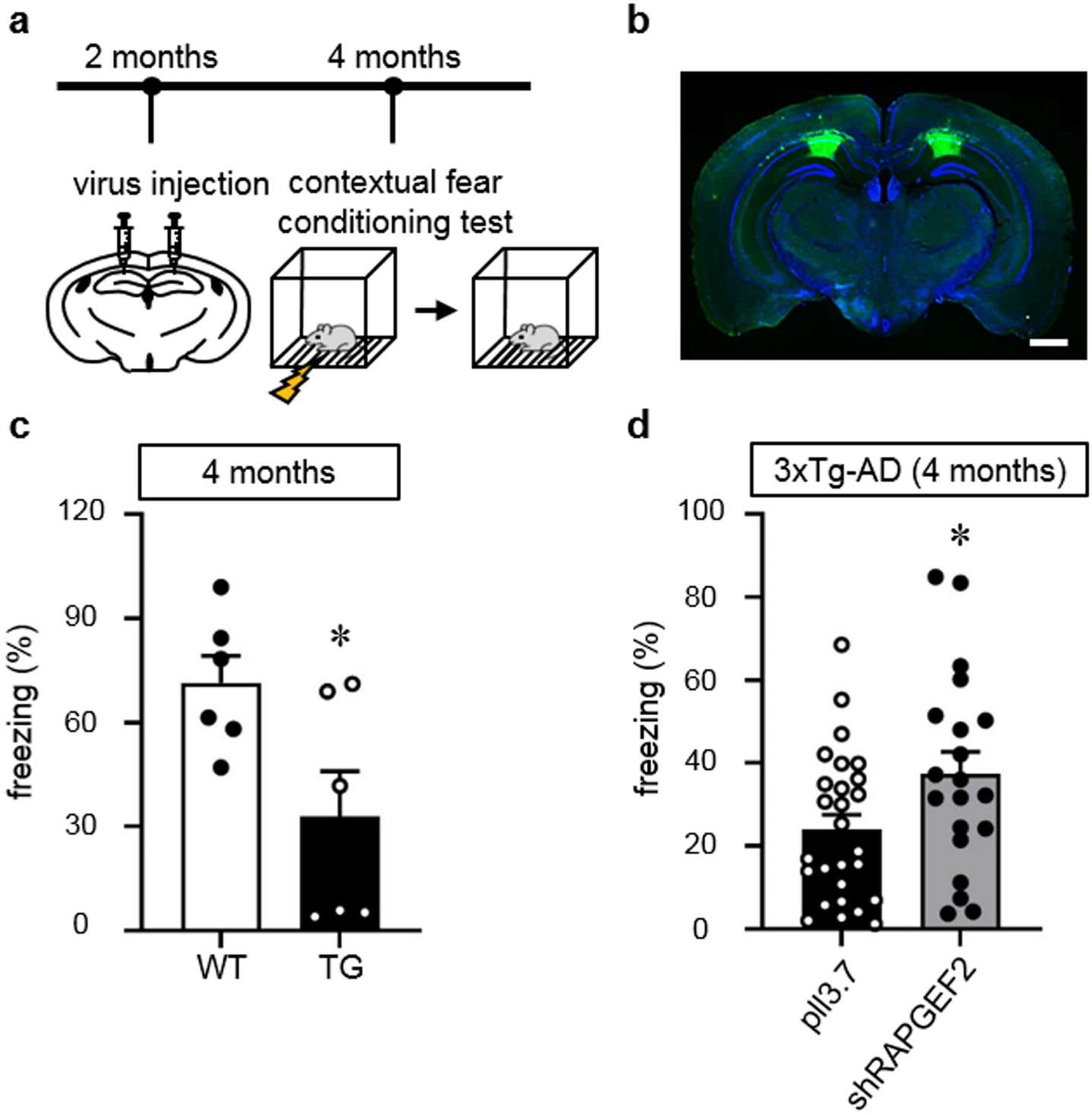

Figure 6

Knockdown of RAPGEF2 expression rescues fear memory deficits in 4-month-old 3xTg-AD mice. a, Time course of stereotaxic delivery of lentiviral particles and behavioral tests. b, Representative image of GFP expression in the hippocampal CA1 area. Lentiviral particles simultaneously expressing shRAPGEF2 and GFP were bilaterally injected into the hippocampal CA1 area. Hoechst dye was used to stain neuronal nuclei (blue). c, The contextual fear memory test was performed in 4-month-old wild-type (WT) and 3xTg-AD (TG) mice (n=6). d, Control (pll3.7) or shRAPGEF2-expressing viral particles were injected into the

hippocampal CA1 area in 2-month-old 3xTg-AD mice. After 2 months, the contextual fear memory test was performed (pll3.7, n=27; shRAPGEF2, n=20). All data are shown as the mean ± SEM. *p<0.05; two-tailed unpaired Student's t-test.

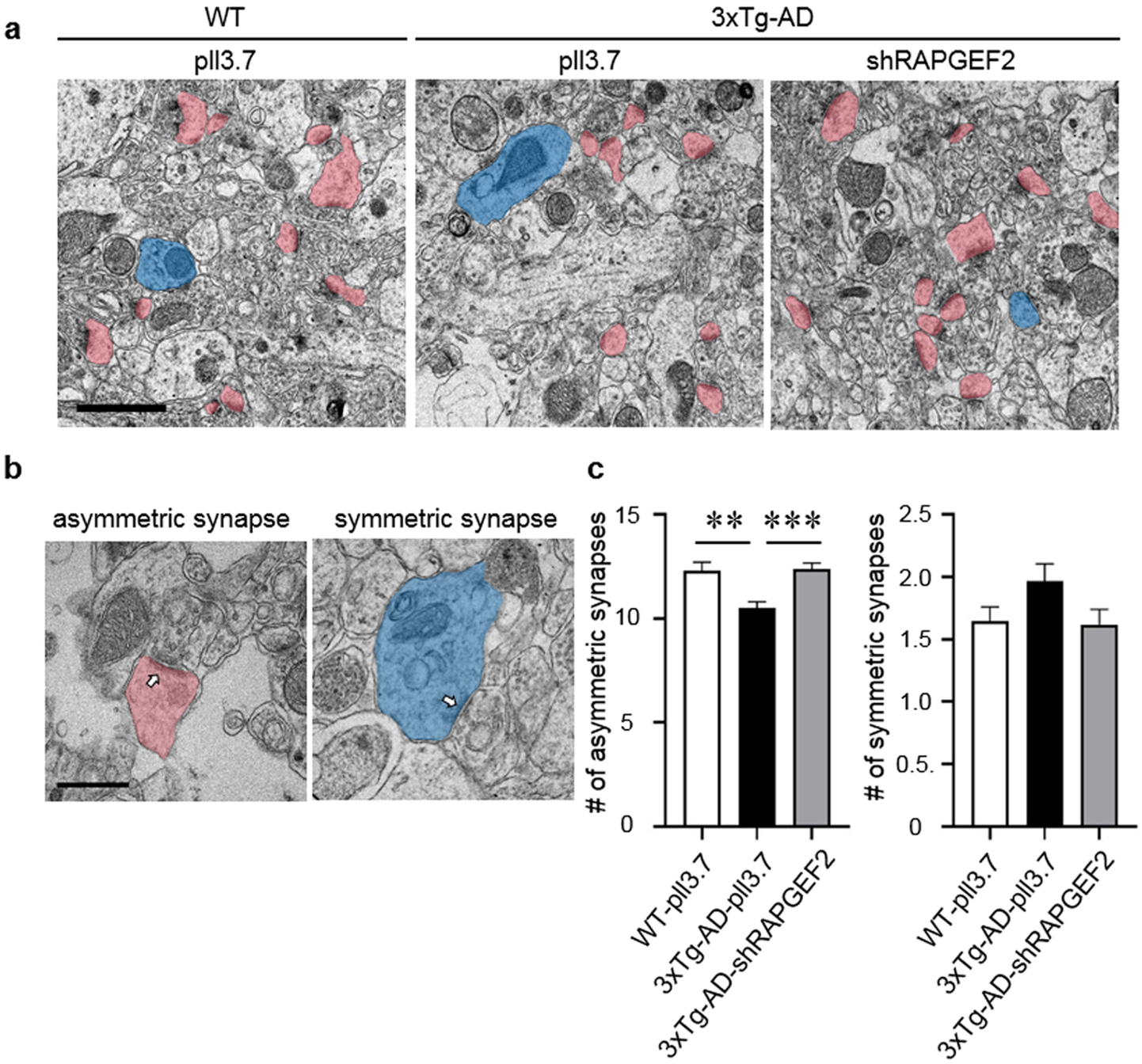

Figure 7

Knockdown of RAPGEF2 preserves excitatory synapse density in 3xTg-AD mice. a, Representative electron microscopic images of the CA1 stratum radiatum of wild-type (WT) and 3xTg-AD mice injected with either control or shRAPGEF2-expressing viral particles. Scale, 1 μm. b, Representative images of asymmetric (left) and symmetric (right) synapses. The arrow indicates postsynaptic density. Scale, 0.5 μm. c, Quantification of the number of asymmetric and symmetric synapses for each condition. The data

are shown as the mean ± SEM (n=90–120 images from 3–4 male mice per group). **p<0.01, ***p<0.001; one-way ANOVA, Tukey's multiple-comparisons test.

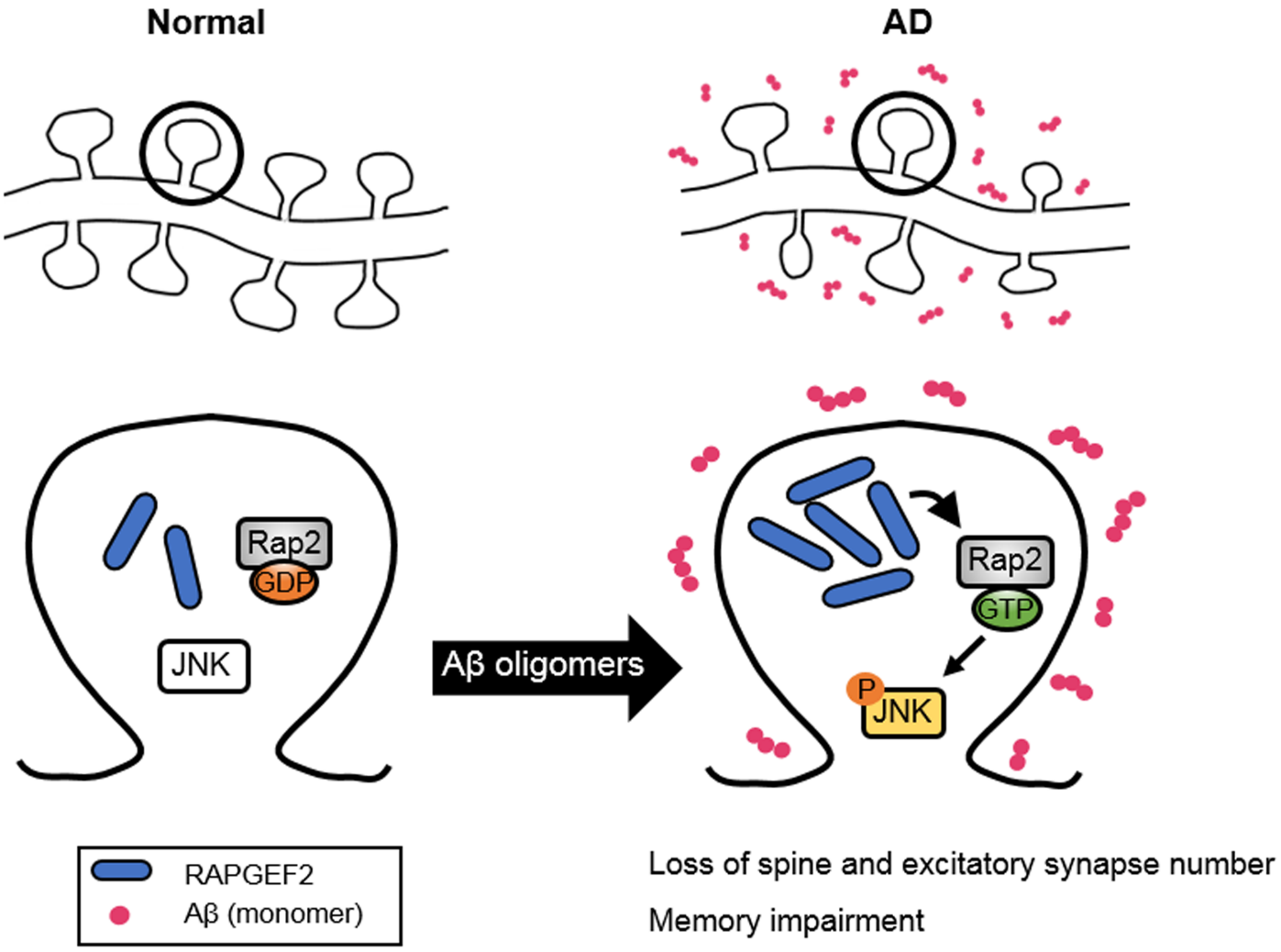

Figure 8

Schematic model for the role of RAPGEF2 in Aβ oligomer-induced synaptic degeneration. In the AD hippocampus (right), synaptotoxic Aβ oligomers stimulate the upregulation of RAPGEF2 levels and lead to the activation of small GTPase Rap2. Rap2 activation, in turn, phosphorylates its downstream signaling target JNK. The Aβ oligomer-mediated upregulation of RAPGEF2 induces the loss of excitatory synapses and subsequent memory impairment.

Supplementary Files

This is a list of supplementary files associated with this preprint. Click to download.

- Additionalfile3.pdf
- Additionalfile4.pdf
- Additionalfile7.pdf

- Additionalfile1.pdf
- Additionalfile2.pdf
- Additionalfile5.pdf
- Additionalfile6.pdf